Rates of OH Radical Reactions. I. Reactions with H_2, CH_4, C_2H_6, and C_3H_8 at 295 K[1]

R. P. OVEREND, G. PARASKEVOPOULOS, AND R. J. CVETANOVIĆ

Division of Chemistry, National Research Council of Canada, Ottawa, Canada K1A 0R9

Received June 20, 1975

R. P. OVEREND, G. PARASKEVOPOULOS, and R. J. CVETANOVIĆ. Can. J. Chem. **53**, 3374 (1975).

A fast flash photolysis kinetic spectrophotometer capable of measuring rates of up to 10^5 s^{-1} is described. The rates of hydrogen abstraction from H_2, CH_4, C_2H_6, and C_3H_8 by OH radicals at 295 ± 2 K, have been measured in the gas phase by hydroxyl resonance absorption spectrophotometry. The influence of secondary reactions on the measured rates and the derivation of the absolute rate constants is discussed in detail.

The absolute rate constants in units of cm^3 mol^{-1} s^{-1} were found to be: $k_{H_2} = 3.49 \pm 0.16 \times 10^9$, $k_{CH_4} = 3.92 \pm 0.16 \times 10^9$, $k_{C_2H_6} = 1.59 \pm 0.10 \times 10^{11}$, and $k_{C_3H_8} = 12.17 \pm 0.63 \times 10^{11}$.

R. P. OVEREND, G. PARASKEVOPOULOS et R. J. CVETANOVIĆ. Can. J. Chem. **53**, 3374 (1975).

Nous décrivons un spectrophotomètre à photolyse-éclair et à cinétique rapide capable de mesurer des vitesses de réaction de l'ordre de 10^5 s^{-1}. Les vitesses d'abstraction des atomes d'hydrogène de H_2, CH_4, C_2H_6 et C_3H_8 par des radicaux OH, à 295 ± 2 K ont été mesurées en phase gazeuse par spectrophotométrie d'absorption de résonance du radical hydroxyle. L'influence de réactions secondaires sur les vitesses mesurées et l'obtention des constantes de vitesse absolues sont discutées en détail.

Nous avons trouvé que les constantes de vitesse absolues en unités de cm^3 mol^{-1} s^{-1} sont: $k_{H_2} = 3.49 \pm 0.16 \times 10^9$, $k_{CH_4} = 3.92 \pm 0.16 \times 10^9$, $k_{C_2H_6} = 1.59 \pm 0.10 \times 10^{11}$ et $k_{C_3H_8} = 12.17 \pm 0.63 \times 10^{11}$.

Introduction

Hydroxyl radicals have long been recognized as being a chain carrier in the oxidative combustion of hydrogen and hydrocarbons; they also play an important role in the chemistry of the upper and lower atmosphere where they act as an oxidant. There is, therefore, a need for accurate values of the rate parameters of the reactions of OH with hydrogen, hydrocarbons, and atmospheric gases for use in numerical modelling of the above processes. Such reactions have been widely studied by various experimental techniques. However, data from earlier studies using flame, shock tube, and flow system experiments showed large discrepancies in the reported values of the kinetic parameters. More recently direct techniques have been developed, using spectroscopic, e.s.r., and resonance fluorescence detection of OH, which have improved the accuracy and precision of the data, so that at present the rate constants of some of the reactions (*e.g.*, H_2, CH_4) are established within a 20% range. The data for OH reactions have been reviewed by Drysdale and Lloyd (1) and Wilson (2), and it appears that further work is necessary, in particular using direct determinations.

In the present paper we describe a fast flash photolysis apparatus coupled with time resolved resonance absorption detection of OH. Signal averaging is employed to improve the signal-to-noise ratio. The apparatus is capable of measuring first order rates of up to 10^5 s^{-1}, thus enabling a more complete range of experimental conditions to be examined than hitherto.

We have in progress an extensive program of study on both abstraction and addition reactions of OH radicals in the gas phase. In this paper, the first of a series, we describe in detail the method used and report the rate constants of abstraction of hydrogen from H_2, CH_4, C_2H_6, and C_3H_8 at room temperature. The reaction of OH + H_2 is much studied and serves as a standard against which we compare our technique. We have also examined the effect of secondary radical reactions on the rate measurements by numerical simulation, and established the conditions for which such an effect is negligible.

[1]Issued as NRCC No. 14847.

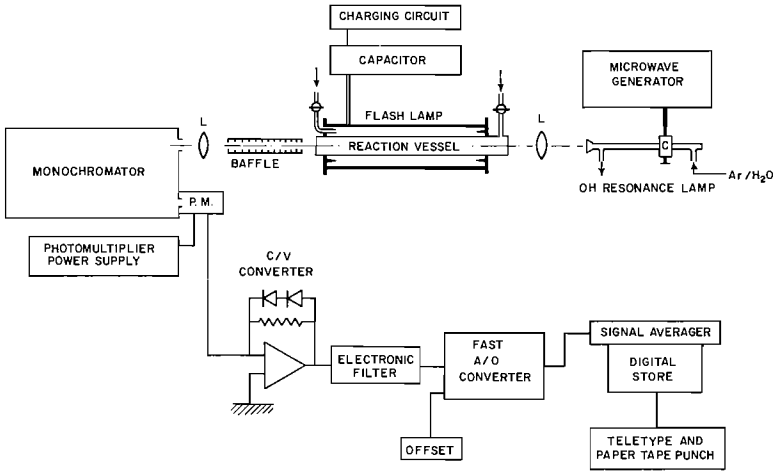

FIG. 1. Block diagram of the apparatus. L, lenses; P.M., photomultiplier; C/V converter, current-to-voltage converter; A/D converter, analog-to-digital converter.

Experimental

The apparatus consists of a fast flash photolysis system coupled with a spectrophotometric detection system. The block diagram of the experimental arrangement is given in Fig. 1. The flash lamp and reaction vessel are a low inductance coaxial assembly based in part on the design concepts of Furumoto and Ceccon (3). The 30 cm length flash discharge is in an annulus 1 mm deep around the 25 mm diameter reaction vessel. The electrodes are polished stainless-steel knife-edged rings. The flash lamp is discharged by lowering the pressure of dry air within the annulus. A range of energies from 100–600 J is obtained by charging either a 1.5 μF or a 5.1 μF capacitor to the appropriate voltage (10–16 kV). With the smaller capacitor the flash peaks at 650 ns and has a decay ($1/e$) time of 850 ns.

Two 50 cm long, 25 mm diameter reaction vessels were used, both made of Suprasil quartz. The first vessel was a simple tube; the second was a double wall tube in which the reaction mixture occupied the 10 mm diameter inner tube and could be surrounded by a suitable optical shield placed in the outer tube.

The OH concentration in the vessel is monitored by following the time resolved attenuation of the OH resonance radiation ($A^2\Sigma^+ \rightarrow X^2\Pi$) produced by a 2.45 GHz microwave discharge in a low pressure ($\sim$1 Torr) Ar/H_2O mixture ($\sim$5% H_2O). The resonance lamp is similar to that described by Carrington and Broida (4). After each flash attenuation of either the Q_1^3 or Q_1^4 rotational lines of the (0,0) band is followed by means of a 1 m Czerny-Turner spectrophotometer (Jarrell-Ash) and a S-5 photo cathode photomultiplier. The spectrometer has a resolution of 0.87 nm/mm and is operated at a band pass of 0.05–0.2 nm.

The photomultiplier voltage divider is wired for fast pulse response and high peak-current capability. The dynode voltage supply is a well regulated high current supply. Together these ensure fast recovery ($\simeq$5–10 μs) after the flash. To further protect the electronics after the photomultiplier from the flash pulse, two high speed signal diodes were wired across the load resistor in the current-to-voltage converter.

The signal is then passed to a variable low pass electronic filter which has a 4 pole Bessel response. The cutoff frequency of the filter was set at $>2\times$ rate to be measured in the experiment; this provides adequate filtering of high frequency noise with a tolerable distortion of the rise to maximum OH absorption. The filtered signal is then accumulated by the fast analog-to-digital (A/D) converter and signal averager combination. Signal averaging techniques are required on account of the low intensity of the resonance lamp and the large electronic instrument bandwidth required to measure rates of $10^5\ s^{-1}$. The signal-to-noise (S/N) ratio of the system is 10 at 1 MHz and 30 at 100 kHz. With signal averaging the S/N ratio improves to 100 with less than 64 flashes.

The main source of OH radicals was the photolysis of water vapor mixed with the reactant and, in a few experiments with H_2 and CH_4, the photolysis of N_2O followed by the reactions:

$$N_2O + h\nu \rightarrow N_2 + O(^1D)$$

$$O(^1D) + H_2 \rightarrow H + OH$$

$$O(^1D) + CH_4 \rightarrow CH_3 + OH$$

The results with both sources of OH radicals were the same within the experimental error.

The gases were handled in a conventional mercury-free vacuum line provided with a Cellows gauge and an oil manometer. The experimental procedure was to prepare an accurately measured mixture made up from the hydroxyl source, the reactant, and the diluent gas (He). The mixture was mixed with a magnetic stirrer before transfer to the reaction vessel, where it was flashed the required number of times to achieve a satisfactory S/N ratio.

The materials were of the highest available purity and in all cases except H_2 and He were subjected to degassing and bulb-to-bulb distillation *in vacuo* before use.

Results

Experiments with varying low water vapor pressures and a constant flash energy showed the expected logarithmic dependence of the maximum OH absorption on the pressure of water, *i.e.*, $\ln I_0/I = KP_{H_2O}$, for absorptions of up to ~40%. The absorption decreased by about 40% when the total pressure in the vessel increased from 100 to 760 Torr; this was attributed to pressure broadening of the rotational line. Trainor and von Rosenberg (5) have discussed in detail the effect of pressure on absorption. In our experiments, in which we measure relative absorption with time, there should be no effect of pressure broadening on the measured rates. In the majority of our experiments the pressure of H_2O was such that the maximum absorption of OH was less than 10%. Using the formula of Kaufman and co-workers (6) and their suggested value of 8×10^{-4} for the oscillator strength of the hydroxyl $A^2\Sigma \rightarrow X^2\Pi$ transition we calculate that 25% absorption in 30 cm path length corresponds to a concentration of $[OH] \approx 1.3 \times 10^{-10}$ mol cm^{-3}. In our experiments the average initial absorption of OH was ~7–12% corresponding to an average concentration of ~$3.3–5.8 \times 10^{-11}$ mol cm^{-3}.

At the wavelengths used >160 nm the OH($X^2\Pi$) is formed without vibrational or rotational excitation (such excited OH, if present, might relax thereby producing an apparent decrease in the measured rates). The absence of OH with vibrational and rotational excitation has been shown experimentally by Welge and Stuhl (7) who found that throughout the 186–140 nm continuum the energy of the photons, in excess of that required to break the H—OH bond appears mainly as translational energy of the H and OH fragments, *i.e.* they found that the intensity of the $v'' = 1$ bands was only a few percent of the (0,0) band, and that the rotational distribution of OH($X^2\Pi$) was practically the room temperature equilibrium distribution.

The alternative source of hydroxyl radicals (*i.e.*, $N_2O + h\nu \rightarrow O(^1D) + N_2$, $O(^1D) + H_2 \rightarrow OH^* + H$) produced results in agreement with those from the photolysis of water. Thus, although the $O(^1D) + H_2$ reaction has been shown to produce vibrationally excited OH^* (8), the excited species have evidently relaxed by the time our measurements commence.

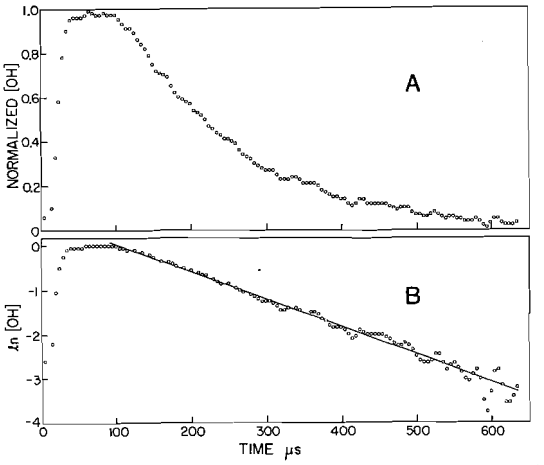

FIG. 2. Example of computer plots of (*A*) normalized [OH], and (*B*) ln [OH] against time for OH + H_2. The conditions of the experiment were: H_2 = 21.36 Torr, H_2O = 2.68 Torr, He = 499.3 Torr, time = 5 μs per channel.

In our experiments the concentration of the second reactant was always made much greater than the initial OH concentration. Under these conditions the reaction is pseudo-first order.

The digital data recorded on the paper tape consist of values of $\Delta I = I_0 - I$ at various time intervals and were processed on an off-line IBM 360 computer. The data were smoothed using a nine-point quadratic approximation suggested by Savitzky and Golay (9). The OH concentration, $[OH] = \ln (I_0/I)$, expressed in normalized

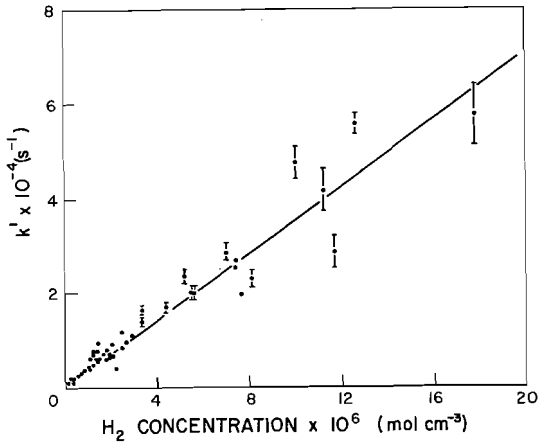

FIG. 3. Plot of pseudo-first order rate constant, k' against the H_2 concentration for the reaction OH + $H_2 \rightarrow H_2O$ + H.

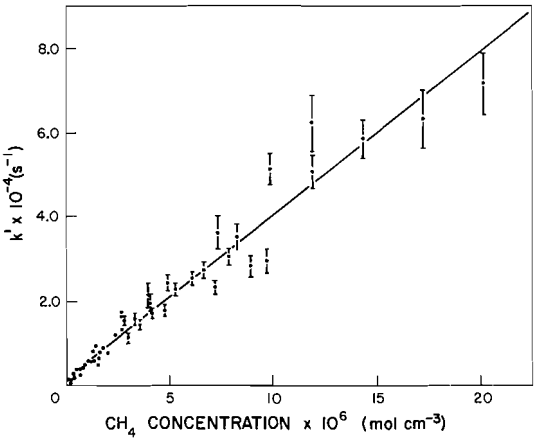

FIG. 4. Plot of pseudo-first order rate constant, k', against the CH_4 concentration for the reaction $OH + CH_4 \rightarrow H_2O + CH_3$.

units (*i.e.* as fraction of the concentration at maximum absorption), as well as $\ln [OH] = \ln (\ln (I_0/I))$ were plotted against time. Such plots are shown in Fig. 2. The latter plots (pseudo-first order plots) were linear over 2–5 half-lives depending on the conditions.

The pseudo-first order rate constant for the OH decay k', was obtained from the slopes of the linear plots. The data had sometimes superimposed on them a sporadic spike noise which occurred in only one direction, as will be illustrated in the next section. The effect was easily filtered out by eye and the slope drawn by hand.

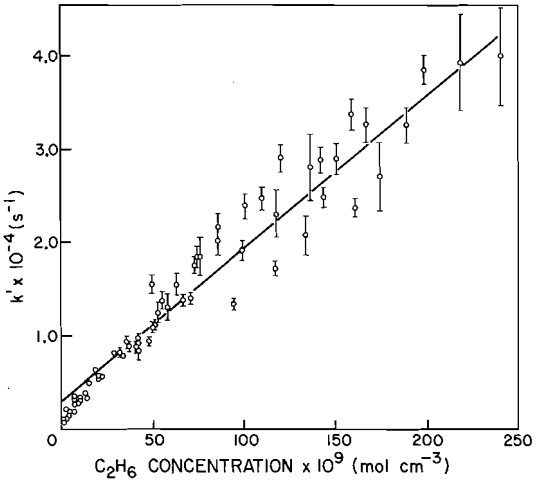

FIG. 5. Plot of pseudo-first order rate constant, k', against the C_2H_6 concentration for the reaction $OH + C_2H_6 \rightarrow H_2O + C_2H_5$.

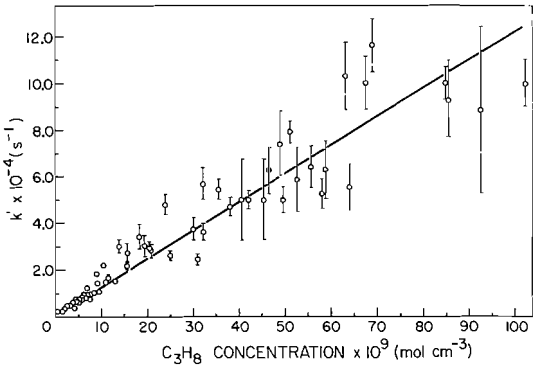

FIG. 6. Plot of pseudo-first order rate constant, k', against the C_3H_8 concentration for the reaction $OH + C_3H_8 \rightarrow H_2O + C_3H_7$.

The pseudo-first order rate constant k' obtained over a range of reactant [RH] concentrations is related to the bimolecular rate constant k by the equation $k' = \alpha + k[RH]$. Plots of k' against [RH] are shown in Figs. 3–6, for RH = H_2, CH_4, C_2H_6, and C_3H_8, respectively. The bimolecular rate constants, k, were evaluated from the slope of these plots. The slopes were obtained from least square fits of the equation $k' = \alpha + k[RH]$ to the points with weights of $1/\sigma^2$ where σ is the error in k' evaluated separately as described below. The least square values of the bimolecular rate constants and the standard deviation of the fit are listed in Table 1.

The total pressure in the experiments with all four reactants was varied between 40 and 760 Torr. The measured rate constants were found to be independent of the total pressure.

The effect of accumulation of reaction products (*e.g.* C_2H_6 in the reaction $CH_4 + OH \rightarrow CH_3 + H_2O$) on the measured rates was considered. The reaction mixture in a representative experiment was irradiated repeatedly and the data collected in consecutive batches of four flashes. Comparison of the signal for the first 4 and last 4 in 32 flashes showed no significant difference. A simple calculation shows that in the

TABLE 1. Bimolecular rate constants of the reaction $OH + RH \rightarrow H_2O + R$ at 295 ± 2 K

Reactant RH	k ($cm^3\ mol^{-1}\ s^{-1}$)	Number of experiments
H_2	$3.4_9 \pm 0.1_6 \times 10^9$	72
CH_4	$3.9_2 \pm 0.1_6 \times 10^9$	60
C_2H_6	$1.5_9 \pm 0.1_0 \times 10^{11}$	42
C_3H_8	$12.1_7 \pm 0.6_3 \times 10^{11}$	59

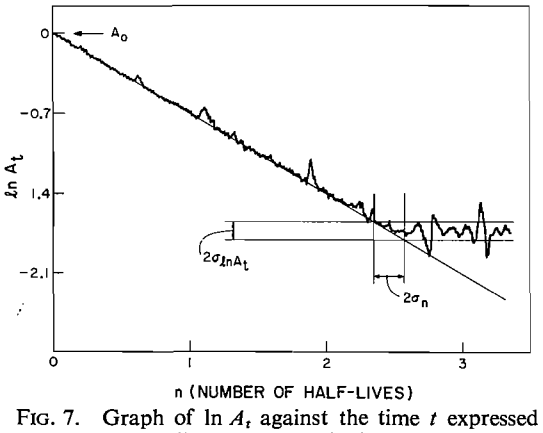

FIG. 7. Graph of ln A_t against the time t expressed as number of half-lives. (The graph shows the unidirectional noise and the error $\sigma_{\ln A_t}$ expressed as uncertainty in the number of half-lives $n \pm \sigma_n$.)

case of CH_4 the effect of accumulation of C_2H_6 from recombination of CH_3 radicals will not perturb the measurements. (It is calculated that after 32 flashes the ratio of the rate of OH with the accumulated C_2H_6 and with CH_4 is about 5×10^{-3}.) In the case of propane the calculation shows that the accumulation of products could possibly affect the measurements. The test described above was carried out more frequently with propane and the total number of flashes was kept at a minimum.

Evaluation of Error

The method of estimation of the error, σ, of the individual values of pseudo-first order rate constant, k', has been described in detail in Appendix I of ref. 10, and will be outlined only briefly here. As mentioned above the slope $\Delta \ln [OH]/\Delta t$ of the graph of the decay curve of ln [OH] against time expressed as number of half-lives and shown in Fig. 7 was drawn by hand. Figure 7 shows also the previously mentioned sporadic unidirectional noise. The error in the slope can be determined from the two extremes of the line

$$k' = \Delta(\ln [OH])/\Delta t = \ln (A_0/A_t)/\Delta t$$

where A_0 = absorbance at $t = 0$, A_t = absorbance at $t = t$, and $\Delta t = t - t_0$ or

$$R_f = \Delta t \times k' = \ln (A_0/A_t)$$

where R_f is defined as rate function. By determining or assessing the experimental precisions at each stage of the measurement of the quantities on the graph of ln A_t against t and using the propagation of error equation we obtain (10)

$$\sigma_{A_t}^2 = \exp(-1.4n)[\sigma_{A_0}^2 + (0.693 A_0 \sigma_n)^2]$$

where n = the number of half-lives over which the straight line in Fig. 7 fits the experimental line; σ_n was estimated from the experimental plots. Graphs of fractional error σ_{R_f}/R_f at constant n's against A_0 are shown in Fig. 8. It may be seen from the graphs that the fractional error, *i.e.*, precision of the pseudo-first order rate constant, k', is $\sim 3\%$ for high A_0 and good straight lines of several half-lives. On the other hand a low A_0 and low n combine to give very poor precision. The errors in k' are shown as error bars of length 1σ in Figs. 3–6.

The time base of the ADC/signal averager was calibrated with an accurate frequency standard. The accuracy is about 1 part in 10^4. The measurement of pressures and concentrations was considered to be both accurate and precise to about 1%. Under these conditions the contribution of these sources to the overall error in the bimolecular rate constant k (evaluated from the slope of the plot of k' against concentration, [RH]) is negligible in comparison to that of spectrophotometry. The overall precisions of the bimolecular rate constants in Table 1 are 10–15% at one standard deviation. The accuracy

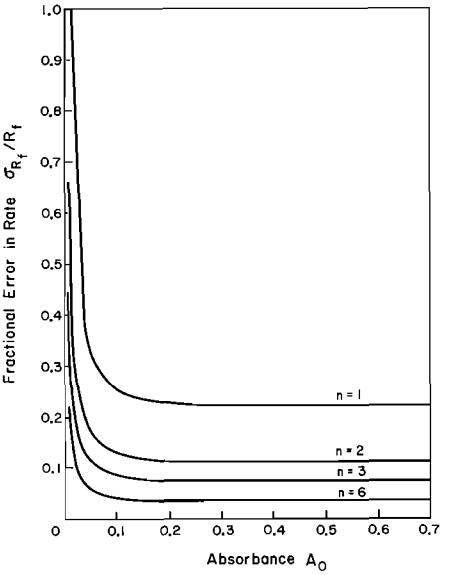

FIG. 8. Graphs of fractional error σ_{R_f}/R_f at constant n against initial absorbance, A_0, for various values of n. (The graphs illustrate the variation of the fractional error with A_0 and with the number of half-lives n.)

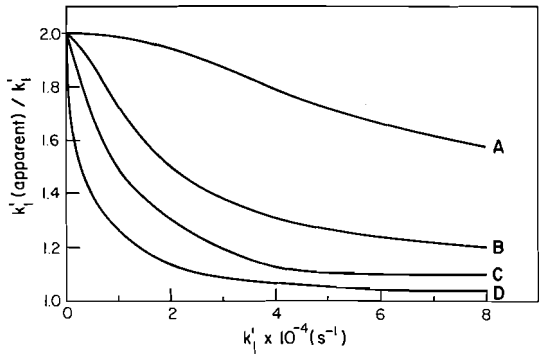

FIG. 9. Effect of the initial OH concentration on the dependence of the k_1'(apparent)/k_1' ratio on k_1' (*i.e.* on the RH concentration) at constant k_2. (The curves were calculated for $k_2 = Z$ (collision frequency) and initial [OH] in mol cm^{-3}: (*A*), 5×10^{-10}; (*B*), 10^{-10}; (*C*), 5×10^{-11}; and (*D*), 2×10^{-11}.)

was estimated to be in the region $\pm 5\%$; this value was estimated from the influence of the flash period, electronic bandwidth, system linearity, and A/D converter resolution on the measured rates.

Discussion

The following reactions were considered for the discussion and interpretation of our experimental results

$$H_2O + h\nu \rightarrow OH + H$$

[1] $$OH + RH \rightarrow H_2O + R$$

[2] $$OH + R \rightarrow \text{Products}$$

[3] $$OH + OH + M \rightarrow H_2O_2 + M$$

[4] $$OH + H + M \rightarrow H_2O + M$$

[5] $$OH + OH \rightarrow H_2O + O$$

where RH = H_2, CH_4, C_2H_6, and C_3H_8. We will examine first if (and to what extent) side reactions of OH affect our results and then we will compare them with other results in the literature.

Effect of Radical–Radical Reactions of OH

The effect of the radical–radical reactions of OH, reactions 2, 3, 4, and 5, was tested by a numerical simulation model in which the differential equations describing the system were integrated numerically for the following initial conditions: (*1*) Since [RH] is present in large excess over OH, reaction 1 was taken as a first order reaction of the form $-\text{d[OH]}/\text{d}t = k_1'[\text{OH}]$ where $k_1' = k_1[\text{RH}]$, and k_1' was varied in the model over a range 10^3 to 10^5 s^{-1}. (*2*) The rate of reaction 2 was taken initially to be the collisional rate. (*3*) Other rate constants were taken from the reviews of Drysdale and Lloyd (1) and Wilson (2). (*4*) The initial concentration of OH radicals was taken to be that estimated earlier using the value of 0.8×10^{-3} for the oscillator strength of OH.

The simulation results showed for measured pseudo-first order rate constants larger than 5×10^3 s^{-1} a negligible influence of radical–radical reactions other than reaction 2, *i.e.* the influence of reactions 3, 4, and 5 was negligible. The plots of ln [OH] against t were curved only in the time region below 5×10^3 s^{-1} showing a second order contribution from reactions 3 and 4. Similarly plots of k_1' against concentration in this time region (very low reactant pressures) were not entirely linear for H_2, and the effect became more pronounced for the C_1–C_3 hydrocarbons. In view of this result and in order to speed the numerical calculations a simplified scheme consisting only of reactions 1 and 2 was modelled over the experimental range. In this model a series of values of k_1 and k_2 were used as input to calculate concentrations of OH at various time intervals. It was found that the scheme nearly always produced linear plots of the ln [OH] against time. From these plots apparent pseudo-first order rate constants, k_1'(apparent), were obtained. The simple model results plotted as a ratio, k_1'(apparent)/k_1', against k_1', (*i.e.* against the RH concentration), are shown in Figs. 9 and 10. Figure 9 shows the influence on the ratio of the initial concentration of OH at constant $k_2 = Z$ (Z = collision frequency) and Fig. 10 shows the influence of k_2

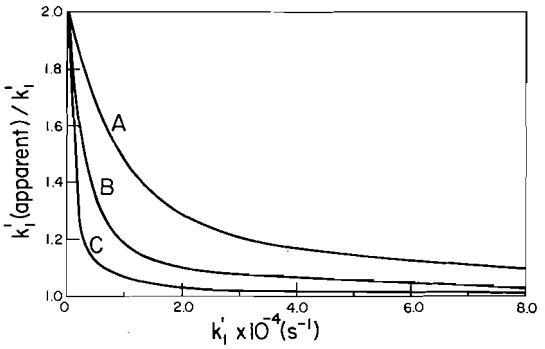

FIG. 10. Effect of the value of k_2 on the dependence of the k_1'(apparent)/k_1' ratio on k_1' (*i.e.* on the RH concentration) at constant initial OH concentration of 5×10^{-11} mol cm^{-3}. (The curves were calculated for k_2 expressed as fraction of the collision frequency Z, (*A*), $k_2 = Z$; (*B*), $k_2 = Z/3$; (*C*), $k_2 = Z/10$.)

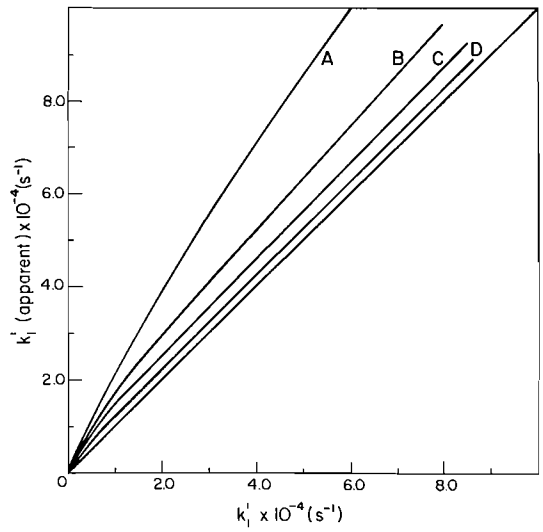

FIG. 11. Dependence of k_1'(apparent) on k_1' (*i.e.* on the RH concentration) at different initial OH concentrations and constant $k_2 = Z$. (The lines were calculated for $k_2 = Z$ and initial OH concentration in mol cm^{-3}; (*A*), 5×10^{-10}; (*B*), 10^{-10}; (*C*), 5×10^{-11}; (*D*), 2×10^{-11}.)

on the ratio at a constant initial concentration of [OH] = 5×10^{-11} mol cm^{-3}. Thus, the simple model indicates that at high measured rates and low initial concentrations of OH the ratio is close to unity, *i.e.* the measured rates will not be appreciably affected by reaction 2. On the other hand at low overall rates and high initial OH concentrations the model predicts an apparent rate increase by almost a factor of two, *i.e.* the plot of the pseudo-first order rate *vs.* concentration is still linear but the slope is almost twice the true bimolecular rate, since the radical R can be considered to be in a steady state. This is illustrated in Fig. 11, where k_1'(apparent) is plotted against k_1', for $k_2 = Z$ and at various values of the initial OH concentration. It may be seen in Fig. 11 that for OH concentrations of 2–5 $\times$ 10^{-11} mol cm^{-3} and rates larger than 5–10 $\times$ 10^3 s^{-1} the lines are almost parallel to the 45° line, *i.e.*, for these conditions the measured slopes are not affected. Subsequent experiments with propane verified this behavior. The general behavior of the series H_2 to C_3H_8 suggests that the rate of reaction of the smaller radicals with OH, *i.e.*, k_2 may be appreciably smaller than that of the propyl radical. The combination of low measured rates and high initial OH concentration, is probably the reason that the rates of OH with CH_4 and C_2H_6 obtained by Horne and Norrish (11) are almost a factor of two larger than the currently accepted values.

Similar considerations apply to the measurement of OH rate constants by the resonance fluorescence technique, where the bimolecular rate constant is obtained from plots of k_1' *vs.* the concentration of RH. A single simulation was made using typical experimental conditions of this technique (12, 13) (*i.e.* initial [OH] = 5×10^{-13} mol cm^{-3} and k_1' = 25–300 s^{-1}). The simulation indicated that k_1'(apparent)/k_1' assumes values close to 2 for low k_1', but decreases with increasing k_1' and approaches 1 at high k_1'.

In the OH concentration range of the present work, the points corresponding to small concentrations of RH on the plots of the first order rate constant *vs.* RH concentration will indicate twice the true bimolecular rate constant, but as the RH concentration increases will gradually assume the true value. Plots of bimolecular rate constants against the RH concentration served to indicate the concentration region in which the points have a large dependence on RH concentration, and these points were not used in the evaluation of the slope so that the measured slopes correspond closely to the true value of the bimolecular rate constant. As a result the small intercepts in Figs. 3–6 cannot be ascribed to a single predominant cause. In the two limiting cases the intercept should be zero, *i.e.* when re-

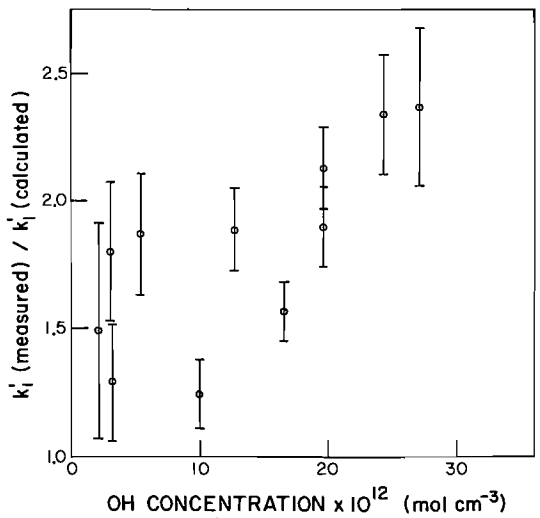

FIG. 12. Variation of k_1'(measured)/k_1'(calculated) with the OH concentration, for k_1'(calculated) of 1.53 $\times$ 10^3 s^{-1} (*i.e.* $k_1 = 12.17 \times 10^{11}$ and [C_3H_8] = 1.26×10^{-9} mol cm^{-3}.)

TABLE 2. Comparison of the room temperature rate constants for the reaction RH + OH → H_2O + R determined by different techniques

	k (cm^3 mol^{-1} s^{-1})		
Reactant	This work	Literature values	Reference
H_2	$3.49 \pm 0.16 \times 10^9$	$3.96 \pm 1.2 \times 10^9$	2
		$3.92 \pm 0.78 \times 10^9$	17
		$4.28 \pm 0.64 \times 10^9$	12
		$4.60 \pm 0.46 \times 10^9$	18
		$4.28 \pm 0.60 \times 10^9$	19
		$4.20 \pm 0.42 \times 10^9$	20
CH_4	$3.92 \pm 0.16 \times 10^9$	$6.85 \pm 4.80 \times 10^9$	2
		$4.51 \pm 0.06 \times 10^9$	13
C_2H_6	$1.59 \pm 0.10 \times 10^{11}$	1.61×10^{11}	2
		$1.79 \pm 0.17 \times 10^{11}$*	16
C_3H_8	$12.17 \pm 0.63 \times 10^{11}$	$6.81 \pm 0.67 \times 10^{11}$*	16
		$5.10 \pm 1.0 \times 10^{11}$	21
		$13.25 \pm 3.6 \times 10^{11}$	22

*These values are our estimates of the weighted means of the corrected rate constants, at room temperature, given in Table II of ref. 16; the weights w were taken to be equal to $1/\sigma^2$ where σ is the reported error of each rate constant.

action 2 causes no interference, and when the concentration of the radical R is in steady state.

Examination of Fig. 9 shows that at a low true rate k_1', for example a rate of 2–3 × 10^3 s^{-1}, the dependence of k_1'(apparent)/k_1' on the concentration of [OH] will be very marked. Figure 12 shows results for propane in this region. The trend in increasing relative rate with OH concentration is evident. The large error bars reflect the difficulty of the measurements at low OH concentrations (*i.e.* poor *S/N* ratios). The apparent trend of the ratio k_1'(measured)/k_1'(calculated) to a value larger than 2 may well be correct, as the simple model discussed above may have shortcomings in this concentration/rate region.

The values of 2–2.5 for the measured to calculated ratio of k_1' led us to consider that photolysis of propane was producing an excessive initial concentration of radicals. In the case illustrated in Fig. 12 where the concentration of propane is 1.26×10^{-9} mol cm^{-3} and that of OH is 25–30 × 10^{-12} mol cm^{-3}, the reported absorption coefficients of propane (14) and water (15) and the path length suggest that the extent of propane photolysis and thus the concentration of radicals formed will be less than 0.001% of the total OH produced (*i.e.* less than 3 × 10^{-16} mol cm^{-3}). This would make a negligible contribution to the rate in the presence of 1.26×10^{-9} mol cm^{-3} of propane.

Comparison of Rate Constant Values

As mentioned in the introduction the reactions of OH with hydrogen and hydrocarbons have been studied widely by a variety of indirect and direct techniques. Prominent among the direct studies is the pioneering work of Greiner (ref. 16 and references therein) who used the flash photolysis kinetic spectroscopy technique. The rate constant of the H_2 reaction, in particular, is more reliably known and is used to test our technique. On the other hand there are few direct determinations of rate constants for the C_2H_6 and C_3H_8 reactions. The rate constants determined in this work together with literature values are given in Table 2. The first entry for H_2, CH_4, and C_2H_6 is the recommended value from the review of Wilson (2), the second entry for H_2 is from the review of Baulch *et al.* (17). Both reviews have summarized work up to 1972; the other entries are values reported after that date.

Our values for H_2 and CH_4 although somewhat lower are, within experimental error, in reasonable agreement with those in the literature. The value for C_2H_6 agrees well with both the recommended value and the value of Greiner (16). The reported values for C_3H_8 (16, 21, 22) differ by over a factor of 2. Our value agrees well with the higher value of Gorse and Volman (22), determined indirectly, relative to the rate constant of the reaction OH + CO.

The authors are grateful to Drs. A. R. Gibbons and H. A. Wiebe for the early work on the development of the apparatus.

1. D. D. DRYSDALE and A. C. LLOYD. Oxid. Combust. Rev. **4**, 157 (1970).
2. W. E. WILSON, JR. J. Phys. Chem. Ref. Data, **1**, 535 (1972).
3. H. W. FURUMOTO and H. L. CECCON. Appl. Opt. **8**, 1613 (1969).
4. T. CARRINGTON and H. P. BROIDA. J. Mol. Spectrosc. **2**, 273 (1958).
5. D. W. TRAINOR and C. W. VON ROSENBERG, JR. J. Chem. Phys. **61**, 1010 (1974).
6. D. M. GOLDEN, F. P. DEL GRECO, and F. KAUFMAN. J. Chem. Phys. **39**, 3034 (1963).
7. K. H. WELGE and F. STUHL. J. Chem. Phys. **46**, 2440 (1967).
8. N. BASCO and R. G. W. NORRISH. Proc. R. Soc. (London) Ser. A, **260**, 293 (1961).
9. A. SAVITSKY and M. J. E. GOLAY. Anal. Chem. **36**, 1627 (1964).
10. R. J. CVETANOVIĆ, R. P. OVEREND, and G. PARASKEVOPOULOS. *In* Proceedings of the Symposium on Chemical Kinetics Data for the Lower and Upper Atmosphere. *Edited* by S. W. Benson. Int. J. Chem. Kinet. Supplement to Vol. 7, 249 (1975).
11. D. G. HORNE and R. G. W. NORRISH. Nature (London), **215**, 1373 (1967).
12. F. STUHL and H. NIKI. J. Chem. Phys. **57**, 3671 (1972).
13. D. D. DAVIS, S. FISCHER, and R. SCHIFF. J. Chem. Phys. **61**, 2213 (1974).
14. H. OKABE and D. A. BECKER. J. Chem. Phys. **39**, 2549 (1963).
15. K. WATANABE, M. ZELIKOFF, and E. C. Y. INN. Absorption coefficients of several atmospheric gases. Geophysics Research Directorate, Air Force Cambridge Research Center, Cambridge, Mass., Technical Report No. 53-23, 1953.
16. N. R. GREINER. J. Chem. Phys. **53**, 1070 (1970).
17. D. L. BAULCH, D. D. DRYSDALE, D. G. HORNE, and A. C. LLOYD. Evaluated kinetic data for high temperature reactions, Vol. 1. Butterworths, London. 1972. p. 77.
18. A. A. WESTENBERG and N. DE HAAS. J. Chem. Phys. **58**, 4061 (1973).
19. I. W. M. SMITH and R. ZELLNER. J. Chem. Soc. Faraday Trans. 2, **70**, 1045 (1974).
20. R. ATKINSON, D. A. HANSEN, and J. N. PITTS, JR. J. Chem. Phys. **62**, 3284 (1975).
21. J. N. BRADLEY, W. HACK, K. HOYERMANN, and H. G. WAGNER. J. Chem. Soc. Faraday Trans. 1, **69**, 1889 (1973).
22. R. A. GORSE and D. H. VOLMAN. J. Photochem. **3**, 115 (1974).